 SDHM, vol.9, no.3, pp.233-252, 2013

Damage Extension Diagnosis Method for Typical Structures of Composite Aircraft Based on Lamb Waves

Dongyue Gao[1], Yishou Wang[1], Zhanjun Wu[1] and Rahim Gorgin[1]

Abstract: In this study, a Lamb wave-based damage extension diagnosis method to monitor the damage on typical structures of composite aircraft is proposed. First, an overview of the damage extension diagnosis method is given. In the method, probability-based damage diagnostic imaging was combined with empirical threshold value to distinguish damage location and estimate damage size in damage extension process. To validate the effectiveness of method, extension diagnosis of simulate delamination damage in typical structure on aircraft were processed. To illustrate the capability of the damage extension diagnostic method, a delamination growth monitoring experiment was performed in a typical reinforce component (T-joint reinforced plate) of composite aircraft during static load testing. The results show that, using Lamb waves-based damage extension diagnosis method, the damage location and size were evaluated accurately; delamination size growth can be monitored by continuous damage extension diagnosis, the monitoring result correspond with destroy law of composite component and the presented size extension indicator correspond with NDT result.

Keywords: structural health monitoring, Lamb waves, damage extension diagnostic method, composite aircraft structures.

1 Introduction

In recent decades, fiber-reinforced composite materials have been extensively used for aircraft structure, due to their high strength-to-weight ratios as well as the advantage offered in aero elastic tailoring [Qing (2006)]. However, potential delamination degradation, flaws and damage can have a detrimental effect on the integrity of the composite aircraft structures strength. These defects may further accumulate or propagate due to external dynamic loading, resulting in catastrophic failure if not

[1] State Key Laboratory of Structural Analysis for Industry Equipments, School of Aeronautics and Astronautics, Dalian University of Technology, Dalian 116024, Liaoning, China.

diagnosed in time [Ihn and Chang (2008)]. Therefore, effective damage evaluation technology of composite aircraft is an essential part of regular aircraft maintenance.

Each of existing traditional non-destructive inspection (NDI) techniques [Savaidis (2013)], ranging from a simple tap test to more complicate ultrasonic or thermography techniques, is limited in efficiency and applicability [Zhou and Cheng (2011)]. Also, a significant amount of equipment and expertise is required to perform this type of inspection [Salowitz (2011)]. A widespread need to develop a cost-effective in-service damage extension diagnosis method for composite aircraft is growing for improving efficiency of the aircraft maintenance by providing preliminary assessment of health condition [Giurgiutiu and Soutis (2012)].

Lamb waves have attracted attention of many researchers in view of their applicability to structural health monitoring of thin-walled structures such as primary structural components of aircraft [Zhou and Cheng (2011)]. A spatially distributed array of permanently mounted piezoelectric sensors is one possible configuration for an active ultrasonic approach to structural health monitoring [Michaels, J. (2008)]. Lamb wave generation and propagation in composite plates have been modelled by Khodaei, Z.S., Liu Qu and Aliabadi, M.H. [Khodaei (2013)]. The main advantage of using Lamb waves for damage diagnosis is that they can be excited from actuators on/within the structure (or emitted by the localized active damage inside the structure) at one point on the structure and can propagate a long distance, while the conventional ultrasonic inspection of large structures are very time-consuming because the transducer needs to be scanned over each point of the structure to be monitored. Numerous investigations have explored the sensitivity of Lamb waves for the detection of damage in composite structures [Mustapha (2011)]. Zhongqing Su and Lin Ye examined the propagation properties of fundamental Lamb modes interacted with interlayer delamination through numerical and experimental analyses [Su, Z. and L. Ye, (2004)]. K. Diamanti developed a system of smart devices that could be permanently bonded to the surface of composite structures and monitor the interaction of Lamb waves with defects [Diamanti and Soutis (2004)]. Stefan h Urlebaus used PVDF (Polyvinylidene Fluoride) as a self-sensing actuator of lamb waves in a smart layer which is manufactured by Acellent technologies for ultrasonic inspection of specimens [Hurlebaus, S. and L. Gaul (2004)]. A diagnostic imaging algorithm has been developed based on the probability of damage at each point of the structure measured by the signal reading of sensors in the baseline and damaged structure [Sharif Khodaei, Z. (2014)]. Malinowski presented investigation of a structural health monitoring method for thin-walled parts of structures [Malinowski, Wandowski and Ostachowicz (2012)]. Putkis proposes determination of the stiffness matrix from the measured group velocities, which can be unambiguously measured in any direction [Putkis, and Crox-

ford (2013)]. Mitra and Mujumdar presents a Lamb wave based methodology for damage detection using frequency spectra in thin metallic and composite plates and a more realistic structure like stiffened carbon-epoxy composite panel [Janarthan, Mitra and Mujumdar (2013)].

Numerous investigations have explored the application of Lamb modes for the detection of damage in composite laminates [Sadri (2013); Rama (2012)]. However, less work has been done on the damage extension diagnosis method for composite aircraft structure.

Damage extension diagnosis method includes damage location and severity evaluation (crack length, delamination area, etc.). Using continuous damage extension diagnosis of structure during different loading level, real-time structural health monitoring can be achieved. This is especially important for improving efficiency of the aircraft maintenance.

The objective of this research is to develop a lamb waves-based damage extension diagnosis method using piezoelectric transducer (PZT) sensors for damage locating and damage growth monitoring on aircraft typical structures. In this paper, a semi-empirical damage size extension indicator is presented for damage area extension diagnostic. First, an overview of the damage extension diagnosis method was given, the health monitoring strategy of the large complex composite structures was presented and the damage diagnosis algorithm base on scattering signal energy was developed for damage location and quantitative. Added mass on the plate will change the local elasticity modulus of structure, simulated damage (added mass) diagnosis test on typical structure of aircraft (thin-walled structure) are presented to determine the effectiveness of the method. To illustrate the delamination growth monitoring capability of the damage extension diagnostic method, damage monitoring test in a typical reinforce component (T-joint reinforced plate) of composite aircraft during static load testing are presented. The results show that, using Lamb waves-based damage extension diagnosis method, the damage location and area were evaluated accurately; delamination growth monitoring can be monitored by continuous damage extension diagnosis, the monitoring result correspond with damage evolution rule of the component and the presented size extension indicator correspond with NDT result.

2 Methodology

Damages (including flaw, delaminating and cracking) appear in aging composite aircraft structure when the structures are subject to fatigue and impact. Conventional NDE for structural criticality, such as C-scan and radiographic inspection, or model-based methods, ranging from modal analyses to static parameters iden-

tification, are facing the challenge of compromise between satisfactory estimation accuracy and versatile applicability in practice. The damage extension diagnosis method could be used as the first stage for damage global detection. The results of damage extension diagnosis method will improve the aircraft maintenance efficiency by providing health reference information include damage location and size for NDE technology. Combination with more sensitive NDE techniques, damage characterizes and shapes would be accurately obtained. In primary structural components of composite aircraft structure, Lamb wave techniques have been proven to provide more information about damage type, severity and location than previously tested methods (frequency response techniques), and may prove suitable for damage extension diagnosis method since they travel long distances. Therefore Lamb waves-based technology was applied as the damage detection method in this research.

Lamb waves-based detection method utilizes the distributed sensors network to generate the Lamb wave. When Lamb waves travel through a region which material properties have changed, scattering occurs in all directions and will be receive by sensors network. Using diagnosis method, various features of scattering can be extracted from the captured signal, including time-of-flight (TOF), magnitude and energy, which contain essential information about the damage.

Features extracted from the captured signal that can be linked with damage at different states is termed damage index (DIs). Some literatures presented two representative relationships between DIs extracted from Lamb wave signals and a specific damage parameter [Ihn and Chang (2008)]. Since the damage index utilizes the information of the forward scattered (or directly transmitted) wave, it is limited to provide a line interrogation and assess the damage only near, or in the line of, the actuator–sensor path.

The TOF defined as the time lag between the incident wave and the scattering wave is one of the most straightforward features of a Lamb wave signal for damage identification. In substance it suggests the relative positions among the actuator, sensor and damage. From the difference in the TOF between the damage-scattered and incident waves extracted from a certain number of signals, damage can accordingly be triangulated [Valdes, S. and C. Soutis (2001)]. The success of triangulating damage in terms of TOF is largely dependent on the accuracy of TOF extraction. The complexity of the composite aircraft structure reduces the accuracy of the TOF method.

Lamb wave tomography diagnosis has been developed based on the computed tomography (CT) using X-ray radiography principle which is widely used in clinical applications. In the diagnosis technique, a simple image concerning the damage information (the location, size and shape of the damage) can be reconstructed us-

ing an appropriate image reconstruction technique. However, this method requires a large number of sensors to scan the entire area carefully for image construction, which limits the application for quick damage identification. Therefore Lamb wave tomography diagnosis method is unfit for aircraft structural health monitoring.

Some researchers proposed some DI-based extension diagnostic methods to locate damage by analyzing the scattered waves [1, 2]. The process of damage diagnosis is shown in figure1; first, DI is generated with each pair of actuator-sensor to characterize the damage. Then, monitored region is discretized into matrix and each element (pixel) of the matrix corresponding to a structural point. Meanwhile, interpolation coefficients are estimated for every pixel in monitored region based on the relative distance between actuator-sensor paths and the pixels. Finally, a digital image is created to highlight the area of damage based on where propagating signals are affected by the local damage.

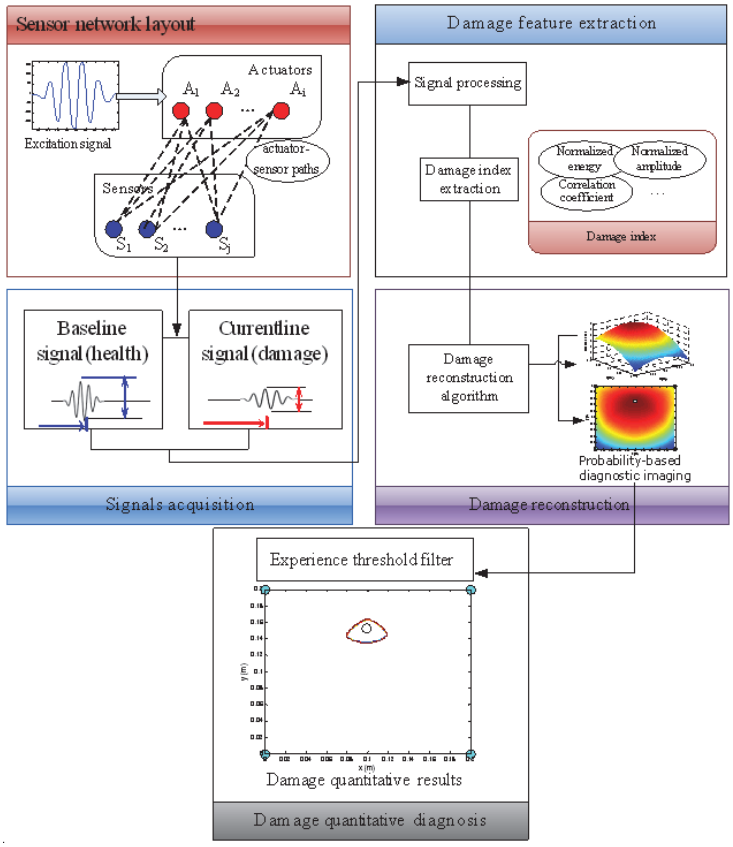

Figure 1: Extension damage diagnosis method.

As shown in figure1, damage extension diagnosis method is divided into three stages: pre-processing stage, extension diagnosis stage and post-processing stage. In the first stage of extension diagnosis method, damage indexes (DIs) of different paths in sensors network were obtained by signal processing and feature extraction; in the second stage of the method, probability-damage region was described by probability-based damage diagnostic imaging method combined with empirical threshold value; in the last stage of the method damage location and severity size extension indicator were outputted as result of damage extension diagnosis method.

Using the sensor network excited lamb wave signal, the monitored region was scanned. Damage indexes (DIs) were obtained by analyzing captured signals of actuator-sensor paths.

The scattering signal energy transmitted along various actuator–sensor paths is shown as follows.

$$DI_{Path(i)} = \sqrt{Eng(scatter)/Eng(base)} \tag{1}$$

Where,$Eng(scatter)$and$Eng(base)$are the energy of scatter signal and baseline signal, respectively. The energy of signals is defined as integration of time-domain signal

Following classical damage imaging method, interpolation coefficients of various paths were utilized to draw damage probability image.

In this work, the monitored region is discretized into a grid of pixels based on the required resolution in X and Y directions. The interpolation coefficient of $Path(i)$ for pixel D is shown as follows.

$$Wn_D = \begin{cases} 1 - \dfrac{R}{h}, R < h \\ 0, R \geq h \end{cases} \tag{2}$$

Where, $R = \frac{L_{A-D}+L_{D-S}}{L_{A-S}}$, L_{A-D}, L_{D-S} and L_{A-S} are distance between the pixel and actuator of $Path(i)$, distance between the pixel and sensor of $Path(i)$ and length of $Path(i)$, respectively.

$(L_{A-D}+L_{D-S})/L_{A-S}$ is referred to as damage relative distance.

Scaling parameter h is employed to control the area influenced by the $Path(i)$. The parameter h is specified as 0.5 in this article. The pixel value is shown as follows.

$$Pv = \sum_{i=1}^{n} DI_{Path(i)} Wn_D \tag{3}$$

Where, n is the amount of actuator-sensor paths. The probability of damage presence at node D is defined by equation (3) and will be projected onto XY plane in

forms of pixel value field, can be illustrated in figure 1. The peak of pixel value field is counted as damage location. Furthermore, in order to quantify damage, some development on this method has been carried out. An empirical threshold T introduced by is shown as follows.

$$T = 0.2[\max(\ pixel \quad value\ ) + \min(\ pixel \quad value\ )] \tag{4}$$

The empirical threshold was installed for every imaging result.

Potential damage region is scaled out by the contour plot. As mentioned above, the monitored region was discretized into matrix and each element (pixel) of the matrix corresponding to a structural point. The damage size can be quantified informally as follows:

$$S_{Damage} = NE_{Non-zero} S_{Region} / NE_{Gloal} \tag{5}$$

Where S_{Damage} and S_{Region} represent the size of the damage and the entire monitored region; $NE_{Non-zero}$ and NE_{Gloal} denote the number of non-zero element and number of the entire element in processed matrix by the threshold alignment, respectively. The semi-empirical size of the damage can be used as a simple size extension indicator. It's important to note that the relation between the semi-empirical size estimation and the physical parameters (e.g. the delamination size) is not fully understood yet, but subsequent tests showing that they have the same change trend. According to the literature [Ihn and Chang (2008)], added mass with a local discontinuity in material thickness and property such as in a case of localized corrosion damage or bonding a substructure will act as a scatter source once impinged by ultrasonic waves. To determine the effectiveness of the method, simulated damage (added mass) location and severity extension test on typical structure of aircraft (thin-walled structure) are presented. To illustrate the delamination growth monitoring capability of the damage extension diagnostic method, damage monitoring test in a typical reinforce component (T-joint reinforced plate) of composite aircraft during static load testing are presented.

3 Applications to structural damage identification

The presented damage diagnostic method was employed to identify damage in two common types of structures: thin-wall structure and CFRP T-joint.

3.1 Diagnosis of added mass damage in thin-wall structure

In order to validate the effectiveness of damage diagnosis method in composite aircraft structure, damage location and size evaluation of bonded added masses damage using damage extension diagnosis method in typical structure on aircraft

(thin-wall structure) were processed. The added masses bonded on the structure are proved to simulate delamination damage by changes in local stiffness.

An aluminum plate (430*500*3 mm) with sensors network and a square mass (20*20*1mm) made of steel is used as experiment specimen. The sensors network consists of four PZT disks (APC851) with diameter of 6.35 mm and thickness of 0.25 mm. The networked sensors were bonded on the specimen using quick-cure epoxy such that they are installed easily and quickly. The material properties of aluminum plate and epoxy layer are listed in Table1, the piezoelectric properties of PZT are listed in Table 2.

Table 1: Mechanical properties of aluminum plate and epoxy layer.

	Young's modulus E (GPa)	Poisson's ratio v	Density $\rho(kg/m^3)$
Plate	70	0.33	2700
Epoxy layer	14	0.31	1400

The locations of sensors and added mass were shown in figure 2.

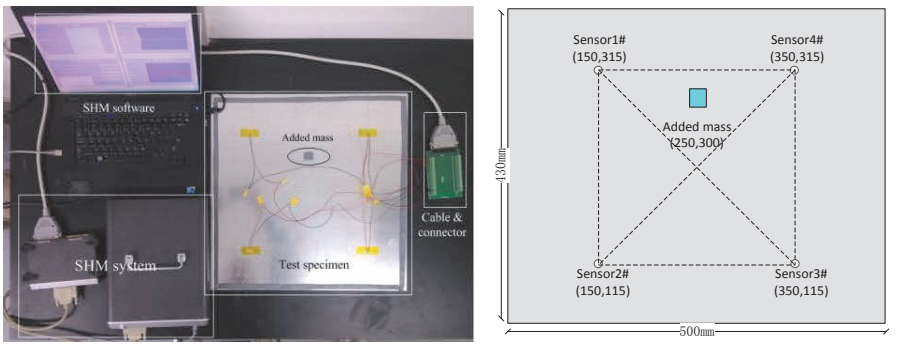

Figure 2: Experiment setup and test specimen.

The damage indexes were evaluated with the sensor measurements from 225 kHz input signals, where it gave the highest signal to noise ratio. A five-peak sine wave modulated by a Gaussian envelope is used to drive actuators because of its narrow-band signal. Signal was generated and captured by damage diagnostic system.

In the experiment PZTs was employed as both actuator and sensor. Each pair of actuator and sensor forms a path. In experiment, PZT sensors were excited in proper sequence, subsequently signal in each path were obtained. Subtraction of the latter from the former measurement yields the scattered wave due to the added

mass. Then, estimate interpolation coefficient for every pixel in monitored region based-on the relative distance between actuator-sensor paths to the pixel; finally, create a digital image to highlight the area of damage based on where propagating signals are affected by the local damage.

Table 2: Material properties of PZT transducer.

Product name	APC 851
Density	7.6
Electromechanical coupling factor	0.71
Relative dielectric constant	1950
Frequency constant	2040
Elastic constant E	63

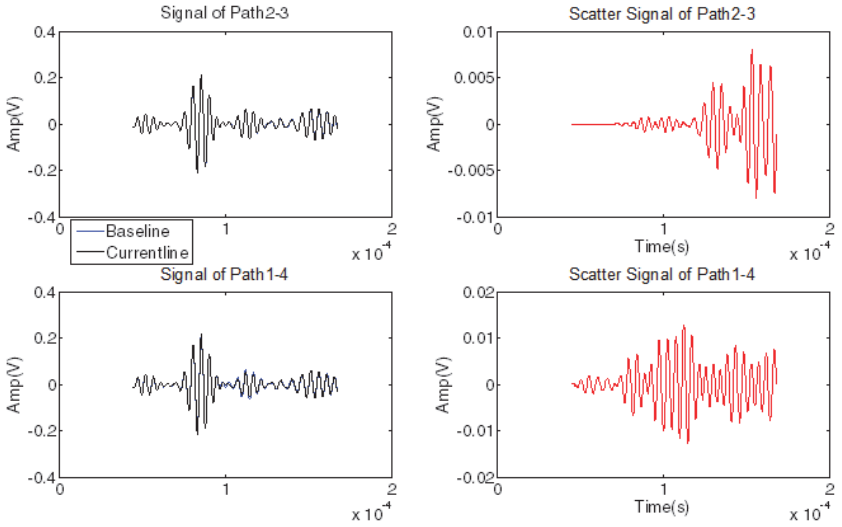

Figure 3: Comparison of typical actuator-sensor paths.

Figure 3 shows the comparison of typical signals at different experiment stages.

In figure 3, blue lines, black lines and red lines represented base signal, current signal and scattering signal which are obtained by subtraction of the latter from the former, respectively. Figure 4 shown the scattering signal of path1-4 is stronger than path2-3. The scattering signal energy transmitted along various actuator-sensor paths was used for monitoring of the added mass location. The damage indexes

are obtained through the equation (1). The normalized damage index of the each actuator-sensor path is shown in figure 4.

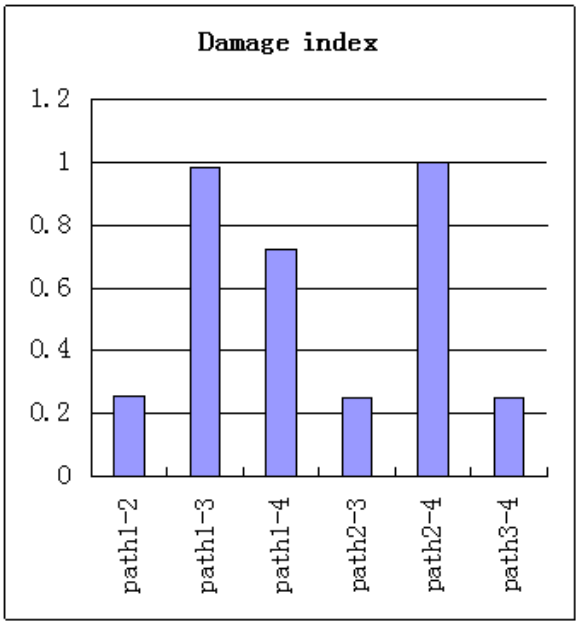

Figure 4: Comparison of Actuator-sensor paths damage indexes.

Damage indexes were extracted from various actuator-sensor paths for establishing different added masses. Figure 4 shows that decreasing relationship between the damage index and damage relative distance. Damage indexes and interpolation coefficients of the entire paths were combined with equation (3), and probability-based diagnostic was achieved.

Applied with the pixel value function defined by equation (3), probability-based diagnostic imaging result for added mass established by paths in the sensor network were fused and the ultimate resulting image is shown in figure 5.

After comparing with the empirical threshold, the diagnostic imaging results were shown as a contour plot in figure 6.

In figure 6, contour plot represent damage region result, white circle was diagnosis location of added mass and red square was used to mark the real location of added mass. The diagnosis location of added mass was (0.099, 0.153), match the real location (0.1, 0.15) well. The extension damage size which could be obtained by equation (4).The damage size, error of result is 2.5%.

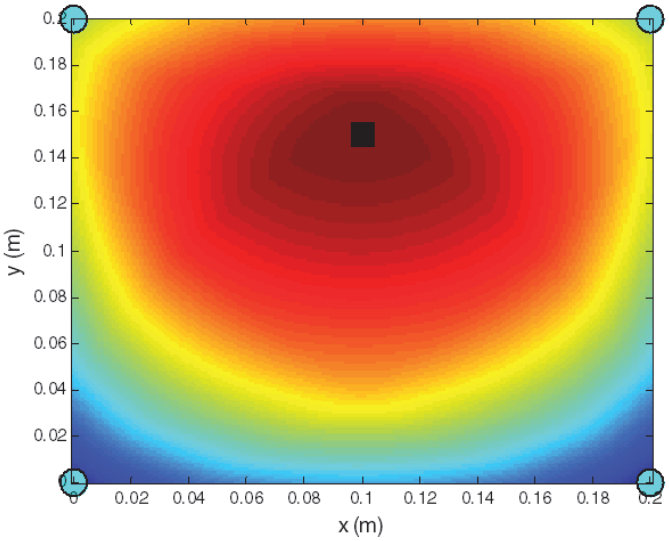

Figure 5: Probability-based diagnostic imaging for added mass.

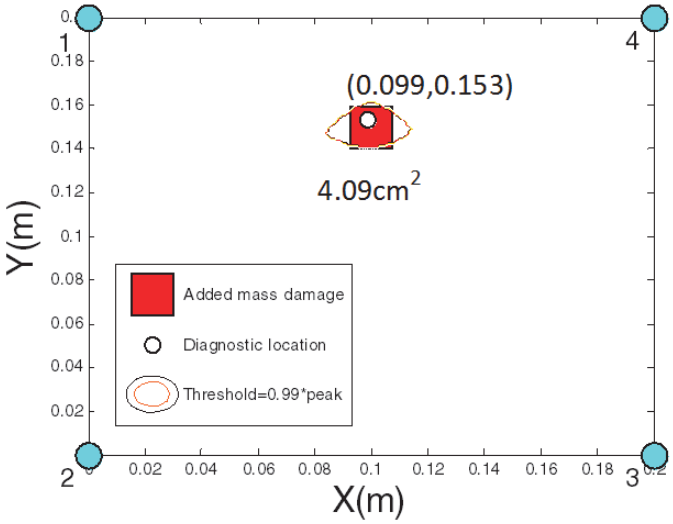

Figure 6: Damage diagnostic results in thin-wall structure.

The experiment result shows that damage location and size were estimated accurately using damage diagnosis method in typical structure on aircraft (thin-wall structure).

3.2 Extension diagnosis of delamination damage growth in T-joint structure

The composite structures have a tendency to delaminate which reduces the strength and stiffness and thus limits the life of a structure. This behavior of composites has caused concern amongst the designers to find the ways to real-time monitoring delamination growth in order to increase the life and the load bearing capability of the structure in service. Real-time monitoring could be achieved by continuous damage extension diagnosis. SHM of full-scale composite horizontal tail under static load has been performed to verify the detection capability of the technology. In order to confirm the correlation between delamination occurring and damage diagnosis results of SHM for the composite horizontal tail structure, we performed a preliminary SHM experiment on a composite T-joint structure under static load. This T-joint structure, as a typical component of composite aircraft structure, can be regarded as a local representative of the full-scale composite horizontal tail.

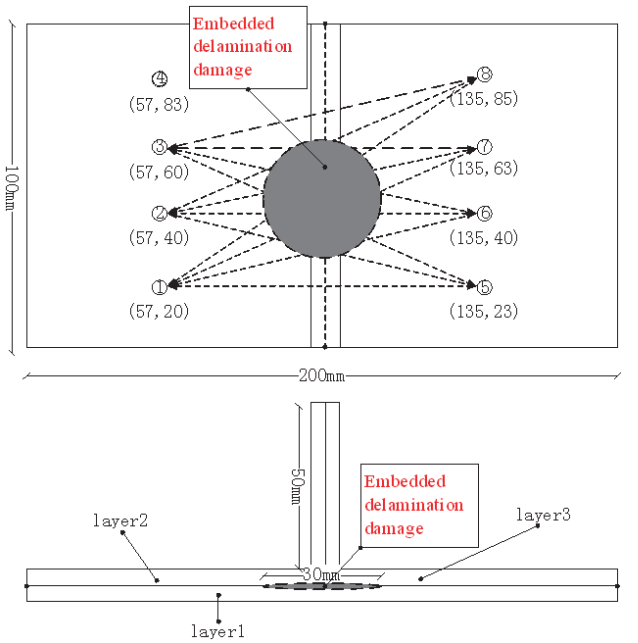

Figure 7: Size of specimen, location of embedded delamination damage and sensors.

As shown in figure 7, T-joint (T700/BA9916 CFRP) reinforced plate (100*200*7 mm) with sensors network and fabricated embedded delamination damage in the center of the specimen. The thickness of each ply is 0.25mm. Lay-up sequences of the T-joint specimen are shown as following:

Layer 1:

[-45/0/45/90/-45/0/90/0/45/90/-45/0/45]

Layer 2:

[45/0/-45/90/45/0/90/0/-45/90/45/0/-45]

Layer 3:

[45/0/-45/90/0/45/0/0/-45/0/45/90/-45]s

The sensors network consists of eight PZT disks (APC851) with diameter of 6.35 mm and thickness of 0.25 mm. The sensors network was bonded on the specimen using quick-cure epoxy, which allowed for quick and easy installation. Size of the specimen, location of embedded delamination damage and sensors are shown in figure 7. The piezoelectric characteristics of PZT are listed in Table 2. The damage indexes of actuator-sensor path are listed in Table 3. The damage index was evaluated with the sensor measurements from 350 kHz input signals, where it gave the minimum attenuation for the specimen. A five-peak sine wave modulated by a Gaussian envelope is used to drive actuators because of its narrow-band signal. Signal was generated and captured by damage diagnostic system.

Table 3: Actuator-sensor path setup in T-joint reinforced plate.

Path No.	1#	2#	3#	4#	5#	6#
Actuator	1	1	1	1	2	2
Sensor	5	6	7	8	5	6
Path No.	7#	8#	9#	10#	11#	12#
Actuator	2	2	3	3	3	3
Sensor	7	8	5	6	7	8

T-joint reinforced rib of the specimen was clamped by tensile testing machine as shown in figure 8. The tension load was increased from 0 to 5kN, and tension load retention was performed at intervals of 1kN. As the tension load increased, the delamination damage growth between the layers.

Data was collected from the sensors network at different load levels. Figure 9 shows the comparison of signals from typical paths at different experiment loading levels.

In figure 9, the blue line in each block diagram represent the signals obtained under different loading level, while the red lines represent distinctions between signal obtained under 0kN loading and signals obtained under a certain loading level, respectively. It is clear that the energy of the scattering signals increases as the tension

Figure 8: Tensile testing machine and T-joint reinforced plate specimen.

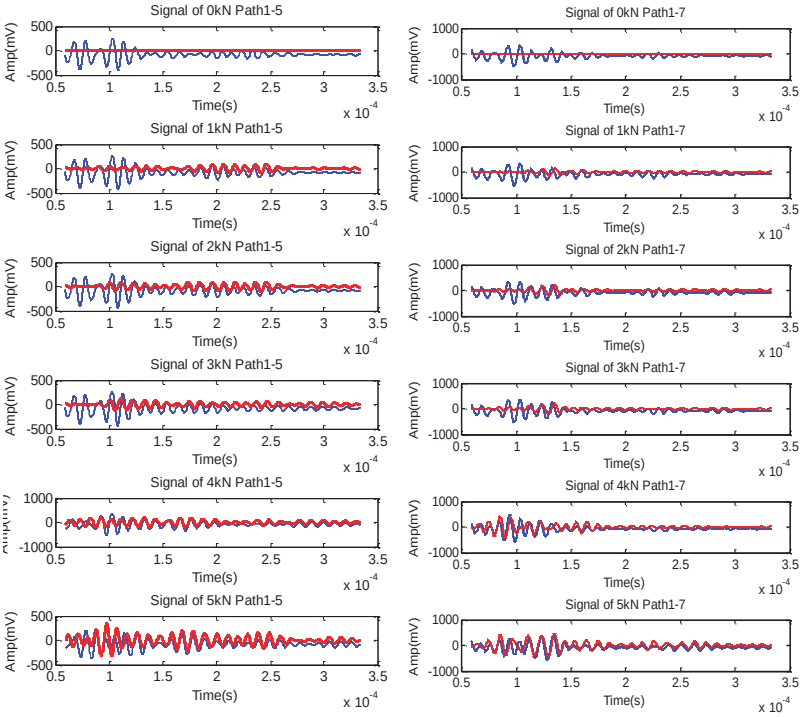

(a). Signal of Path 1-5 (b). Signal of Path 1-7

Figure 9: Typical signals of 200 kHz at different loading levels.

load increase. Once the T-joint reinforced plate complete break, the received signals appeared to have stabilized. Finally, after 5kN loading level, the delamination damage of specimen was detected using ultrasonic C-scanning on the undersurface of the T-joint reinforced plate.

The scattering signal corresponding energy was used to calculate damage index values for each actuator–sensor path. The damage index values of different loading level for each actuator–sensor path were described with bar chart plots as shown in figure 10.

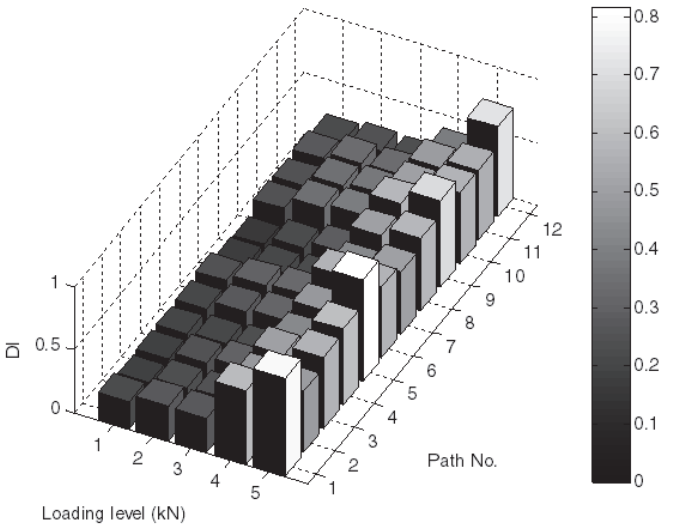

Figure 10: Damage index values bar chart plots.

As shown in Figure 10, the DI of each actuator–sensor path almost tripled when the loading level is rise from 2kN to 3kN. The comparing result show that the maximum DI value always falls on path1-5, 2-5, 3-5, 3-8.

Growth of delamination damage size with the increase of load was quantized using the extension diagnostic imaging method mentioned above. First, under each loading level, probability-based diagnostic imaging was implemented; then, an empirical threshold of last loading level was installed for diagnostic imaging results under different loading levels; subsequently, set pixel value which below the threshold to zero; finally, output the quantify damage size result and the empirical size extension indicator. These images provide a visual representation of the location of structural changes and can be used as a qualitative measure of damage size, as shown in figure 11.

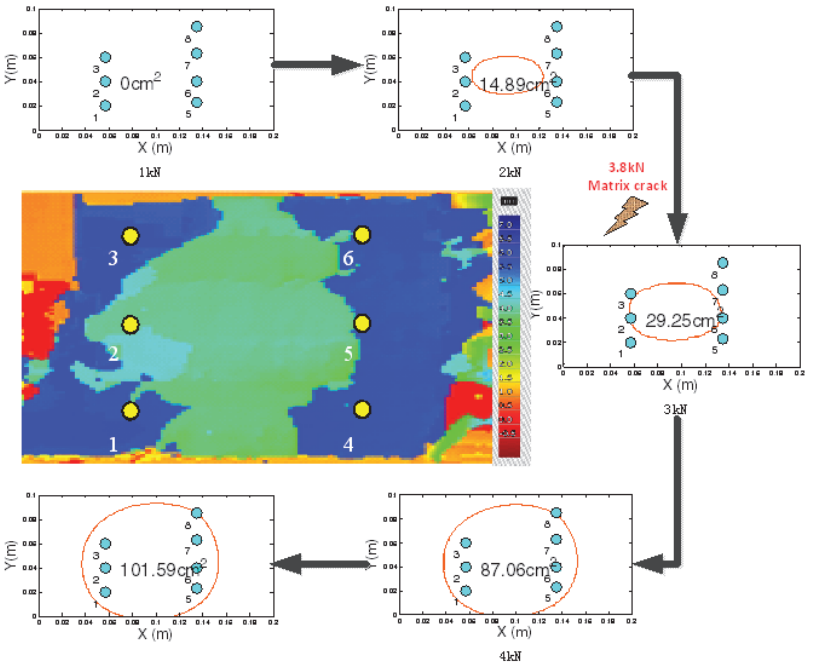

Figure 11: Image of damage growth during tensile test.

The ultrasonic C-Scan test was adopted to measure the delamination damage region after 5kN load. The T-joint specimen after load was scanned in pulse-echo mode by means of a focused ultrasonic probe with a center frequency of 5MHz. During s-canning, the probe emits ultrasonic waves, while the echo signal is recorded at same point, stored on in the hardware of ultrasound scanner. Ultrasonic C-Scan result is shown in center of Figure 11. The pixel color scale of ultrasonic C-Scan result represented echo time of the location, PZT sensors were marked by yellow circles. As shown in Ultrasonic C-Scan result, after 5kN load, the delamination damage extended into 60*76mm. Delamination of 3.5-4.0mm deep complete throughout the T-joint along the stiffener.

As shown in figure 11, the sizes of delamination damages under different loading levels were shown as a cloud chart in extension diagnostic imaging results, respectively. In the ultrasonic C-scan test result after tensile testing, blue zone represents the plate without damage; the green zone represents the delamination damage while the red circles represent sensors. Result of ultrasonic C-scan shown that damage zone exceed sensors network boundary, through the bottom of T-joint rib, the size of the finally delamination is 105cm2.

The damage size can be quantified informally as equation (4). The growth of the damage size under different loading level was shown in figure 12.

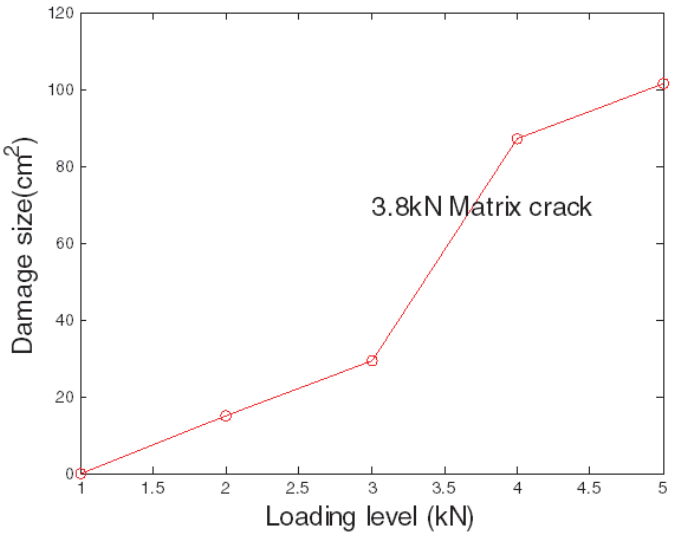

Figure 12: Delamination size extension results of different loading level.

As shown in figure 12, the growth of damage size is very low under 1kN loading level; later, damage size suddenly extended for two times from 29.25cm^2 to 87.06cm^2 after matrix crack occur under 3.8kN loading; finally, damage size tended to be stable, the delamination extension diagnosis size is 101.59cm^2, error of extension result is 3.2%. The extension diagnostic results showed that the extension diagnostic method is extremely sensitive to damage growth and the comparison between C-scan and extension diagnostic results show that the estimates match the actual damage sizes well.

The result of delamination growth monitoring in aircraft typical structure during tensile testing shows that the extension diagnostic method is able to monitor the damage growth and the semi-empirical size extension indicator matches the actual damage sizes well.

4 Conclusions

Lamb waves-based damage extension diagnosis method is proposed in this research. Using damage extension diagnosis method, damage location and size of damage could be obtained. The health condition of the structure can be real-time monitored by processed damage extension diagnosis method continuously during

different loading level. The applicability of damage extension diagnosis method is verified by monitoring the damage location in a thin-walled structure and monitoring the delamination growth during tensile test in T-joint reinforced plate. The damage extension diagnosis algorithm can locate the damage with high accuracy. For growth delamination damage in typical structure of aircraft typical structure, delamination damage growth can be determined well by the size extension indicator.

The results show that, using Lamb waves-based damage extension diagnosis method, the damage location and size were evaluated accurately; delamination growth monitoring can be monitored by continuous damage extension diagnosis, the monitoring result correspond with damage evolution rule of the component and the presented size extension indicator correspond with NDT result.

Acknowledgement: This work was supported by the National Natural Science Foundation of China (11172053 and 91016024) and the New Century Excellent Talents in University (NCET-11-0055) and the Fundamental Research Funds for the Central Universities (DUT12LK33).

References

Diamanti, K.; Hodgkinson, J. M.; Soutis, C. (2004): Detection of low-velocity impact damage in composite plates using Lamb waves. *Structural Health Monitoring,* vol. 3, no. 1, pp. 33-41.

Giurgiutiu, V.; Soutis, C. (2012): Enhanced Composites Integrity Through Structural Health Monitoring. *Applied Composite Materials,* pp. 1-17.

Hurlebaus, S.; Gaul, L. (2004): Smart layer for damage diagnostics. *Journal of intelligent material systems and structures,* vol. 15, no. 9-10, pp. 729-736.

Ihn, J.-B.; Chang, F.-K. (2008): Pitch-catch active sensing methods in structural health monitoring for aircraft structures. *Structural Health Monitoring,* vol. 7, no. 1, pp. 5-19.

Janarthan, B.; Mitra, M.; Mujumdar, P. M.(2013): Lamb wave based damage detection in composite panel Source. *Journal of the Indian Institute of Science,* vol. 93, no. 4, pp 715-734.

Khodaei, Z. S.; Liu, Qu; Aliabadi, M. H. (2013): Influence of adhesive layer on actuation of lamb wave signals. *Key Engineering Materials*, vol. 525-526, pp. 617-20

Michaels, J. (2008): Detection, localization and characterization of damage in plates with an in situ array of spatially distributed ultrasonic sensors. *Smart Mate-*

rials and Structures, vol. 17, 035035.

Malinowski, P.; Wandowski, T.; Ostachowicz, W. (2012): Investigation of sensor placement in Lamb wave-based SHM method. *Key Engineering Materials,* vol. 518, p.p 174-183.

Mustapha, S. et al. (2011): Assessment of debonding in sandwich CF/EP composite beams using A0 Lamb wave at low frequency. *Composite Structures,* vol. 93, no. 2, pp. 483-491.

Putkis, O.; Croxford, A. J. (2013): Stiffness Matrix Determination of Composite Materials Using Lamb Wave Group Velocity Measurements. *Proceedings of the SPIE - The International Society for Optical Engineering,* vol. 8694, pp 869403.

Qing, X. P. et al. (2006): A real-time active smart patch system for monitoring the integrity of bonded repair on an aircraft structure. *Smart materials and structures,* vol. 15, no. 3, pp. N66.

Rama Mohan Rao, A.; Krishna Kumar, S.; Lakshmi, K. (2012): Sensor Fault Detection in Large Sensor Networks using PCA with a Multi-level Search Algorithm. *SDHM: Structural Durability & Health Monitoring,* vol. 8, no. 3, pp. 271-294.

Salowitz, N. et al. (2011): Structural health monitoring of high temperature composites. in Proceedings of the ASME 2011 international mechanical engineering congress & exposition.

Savaidis, G.; Malikoutsakis, M.; Jagenbrein, A.; Savaidis, A.; Soare, M.; Predoi, M. V. ; Soare, A.; Diba, I. C. (2013): Structural Integrity and Health Monitoring of Road and Railway Tanks based on Acoustic Emission. *SDHM: Structural Durability & Health Monitoring,* vol. 9, no. 2, pp. 129-154,

Schmidt, D.; Sadri, H.; Szewieczek, A.; Sinapius, M.; Wierach, P.; Siegert, I.; Wendemuth, A. (2013): Characterization of Lamb wave attenuation mechanisms. *Source: Proceedings of the SPIE - The International Society for Optical Engineering,* vol. 8695, pp 869503.

Sharif Khodaei, Z.; Bacarreza, O.; Aliabadi, M. H. (2014): Lamb-wave based technique for multi-site damage detection. *Key Engineering Materials,* vol. 577-578, pp. 133-136, 2014, Advances in Fracture and Damage Mechanics XII.

Su, Z.; Ye, L. (2004): Fundamental Lamb mode-based delamination detection for CF/EP composite laminates using distributed piezoelectrics. *Structural Health Monitoring,* vol. 3, no. 1, pp. 43-68.

Valdes, S.; Soutis, C. (2001): A structural health monitoring system for laminated composites. in Proceedings of DETC.

Zhao, X. et al. (2011): Ultrasonic Lamb wave tomography in structural health

monitoring. *Smart Materials and Structures,* vol. 20, no. 10, pp. 105002.

Zhou, C.; Su, Z.; Cheng, L. (2011): Probability-based diagnostic imaging using hybrid features extracted from ultrasonic Lamb wave signals. *Smart Materials and Structures,* vol. 20, no. 12, pp. 125005.